Available online on www.ijcpr.com
International Journal of Current Pharmaceutical Review and Research; 7(6); 319-333

ISSN: 0976 822X

Research Article

Electrophoretic and Molecular Dynamic Evaluation of Mutagenicity Induced by Toxic Factors Affecting Testicular Tissue in Rats

Wael M Aboulthana[1*], Mohamed Ismael[2], Hatem S Farghaly[3]

[1]*Biochemistry Department, Genetic Engineering and Biotechnology Division, National Research Centre, 33 Bohouth Street, Dokki, Giza, Egypt affiliation ID: 60014618.*
[2]*Energy and Environmental Sciences Laboratory, Chemistry Department, Faculty of Science, Sohag University, Egypt.*
[3]*Department of Biochemistry, Faculty of Pharmacy, Nahda University, Beni-Sueif, Egypt.*

Available Online:25th December, 2016

ABSTRACT
The testes contain many proteins including testis-specific protein kinase 1 (TESK1) expressed predominantly and ubiquitously in mature testis. They exhibited a vital role in spermatogenesis process. Lithium is an effective drug for the treatment of psychiatric disorders. Lead acetate (Pb_2COOH) and Carbon tetrachloride (CCl_4) which is used as an insecticide in agriculture are considered as environmental pollutants. The prolonged exposure to these (toxic) substances exhibited adverse effect on male reproductive organs. Doxorubicin (DXR) and cyclophosphamide (CYP) are effective chemotherapeutic drugs. They exhibited toxicity on testicular proteins. Irradiation caused disruption of normal cyclic spermatogenesis through radiotherapy. During the present study, these toxic factors affect all electrophoretic patterns at qualitative level through their effect on number and arrangement of the bands and at the quantitative effect through changing the band quantity. In the electrophoretic protein pattern, the lowest similarity index (SI) value (0.42) was recorded with CYP-treated group and the highest SI value (0.79) noticed with Pb_2COOH-treated group. In the electrophoretic lipoprotein pattern, the lowest SI values (0.44) was observed with Pb_2COOH-treated group and the highest SI values (0.73 and 0.80) observed with CCl_4-treated and irradiated groups. In catalase (CAT) pattern, the lowest SI value (0.69) was noticed in DXR-treated, CYP-treated and irradiated groups. The highest SI value (0.91) was observed with Pb_2COOH-treated, Li_2CO_3-treated and CCl_4-treated groups. In peroxidase (Gpx) pattern, the lowest SI value (0.25) was noticed with irradiated group and the hightest value (0.75) observed with CCl_4-treated group. In esterase (EST) pattern, the lowest SI value (0.44) was observed with irradiated group and the highest SI value (0.86) noticed with DXR-treated group. The 3D model of TESK1 was built by means of restraint-based comparative modeling. It was noted that model of the TESK1 was quite big and no available template for the whole sequence and its first half (Up to residue 333).

Keywords: Lithium Toxicity, Carbon Tetrachloride, Lead Toxicity, Doxorubicin, Cyclophosphamide, Irradiation, Testis-specific protein kinase.

INTRODUCTION

The testes contain various proteins necessary for spermatogenesis and development of the reproductive system. These proteins and their mRNA are expressed widely in the mature testes. The protein content was considered as a marker of testicular tissue injury[1]. Lithium is alkali element. It is used as an effective drug for the treatment of several psychiatric disorders in human. The prolonged exposure to lithium during the therapeutic use has several toxic effects leading to various undesirable side effects. It was found that lithium carbonate promoted toxicity and showed adverse effect on male reproductive organs through lowering the fertility index of male rats to 50%[2]. Injection of lithium at the therapeutic doses caused destruction of leydig cells followed by remarkable reduction of sperm viability and motility[3]. This might lead to reducing steroidogenic activity and efficiency of spermatogenesis process in a dose-dependent manner[2,4]. Carbon tetrachloride (CCl_4) is a colorless liquid organic compound. It is well known that it exhibits hepatotoxic and nephrotoxic activities[5]. It is used as an insecticide in agriculture for fumigation of the grains. The industrial workers are susceptible to the particular tissue injury induced by CCl_4 toxicity during their life. It enhance the oxidative stress through generation of the free radicals and oxidation of the macromolecules such as lipids and proteins[5,6]. Lead is a heavy metal belongs to common environmental and occupational pollutants. It is considered an important cause of infertility among occupational workers. It affects the male reproductive organs at the biochemical[7] and physiological level[8]. Low dose of lead was sufficient to arrest spermatogenesis process[9]. Cancer treatment by mean of chemotherapy is not found to be safe due to the side effects of the chemotherapeutic drugs on the healthy tissues[10]. The testicular cells are most sensitive to the chemotherapeutic drugs which influence severely on

**Author for Correspondence: wmkamel83@hotmail.com*

spermatogenesis process[11]. Doxorubicin (DXR) and cyclophosphamide (CYP) belong to numerous chemotherapeutic drugs[12]. The treatment with CYP affects testicular cells through depletion of the differentiated cells in the testis[13]. This results in depletion of germ cells maturation and hence reduction in sperm counts[14,15]. DXR is very active against wide spectrum of cancerous tumors and is mainly used in the treatment of lymphomas, leukemias and other solid tumors[16]. It exhibits dose-dependent toxic effect on different organs[17]. It affected the male reproduction ability through changing the testicular proteins[18]. Also, it influences the testicular lipids which are consisting of very long chain polyunsaturated fatty acids[19]. The radiation exposure by mean of radiotherapy leads to serious systemic damage to various cellular structures[20]. It affected the testicular tissue which represents the most radiosensitive organ through disruption of normal cyclic spermatogenesis process and therefore, impairment of fertility[21,22]. Testis-specific protein kinase 1 (TESK1) is a 626 amino acid serine/threonine kinase. It is a protein kinase with a unique structure consisting of an N-terminal protein kinase domain and a C-terminal proline-rich domain[23]. It was revealed that TESK1 protein exhibited a vital role in spermatogenesis. Its mRNA is expressed predominantly and ubiquitously in the testicular germ cells and it may play an important role in spermatogenesis process[24,25]. TESK1 is a dual specificity protein kinase. It is capable of phosphorylating both serine/threonine and tyrosine residues in its sequence. The autophosphorylation plays a role in regulating the kinase activity of TESK1[26]. The present framework aimed to investigate the different mutagenicity induced by selected toxic substances in the testicular tissue in rats. Various electrophoretic patterns were monitored and compared with control group. The 3D models of the TESK1 were built using homology modeling to give a first insight about the structural characteristics of the activated regions in this protein kinase.

MATERIALS AND METHODS

Materials: Chemicals and Reagents

Acrylamide, Bis-acrylamide, Ammonium persulfate (APS), N, N,N,N-Tetramethylethylnediamine (TEMED), Tris buffer, Coomassie Brilliant Blue G-250 (CBBR-250) and Sudan Black B (SBB) were procured from Sigma-Aldrich. The chemicals used for in-gel esterase staining including α- and β-naphthylacetate, Fast Blue RR were purchased from Qualigens Fine Chemicals, India. Cyclophosphamide (CYP), Doxorubicin (DXR), Lead Acetate Trihydrate (Pb_2COOH), Carbon Tetrachloride (CCl_4), Lithium Carbonate (Li_2CO_3) and Benzidine were purchased from Sigma Chemicals Company (London, UK). All other chemicals and reagents used were of analytical grade and of highest purity.

Animals and Treatment

Healthy seventy adult male Wistar rats (weighing 150–170 g) were housed as 7 groups. The animals were kept under normal conditions at 25 ± 2°C. All the experimental procedures were carried out according to the ethical guidelines and protocol approved by the institutional animal care of National Research Centre, Egypt.

Experimental Design

The rats were randomly divided into 7 groups each containing 10 rats. Group I (Control group): Rats were fed with normal diet as *ad libitum* and received distilled water for 60 days. Group II (Pb_2COOH-treated group): Rats received Pb_2COOH at concentration of 30 mg/kg body weight orally by gavage tube for 60 days by gavage tube[27]. Group III (Li_2CO_3-treated group): Rats were treated with Li_2CO_3 solution interperitoneally (i.p.) at the dose 25 mg/kg B.W./day) for 31 days[28]. Group IV (DXR-treated group): Rats received DXR at dose level of 25mg/kg b.wt for three times per week for two weeks[29]. Group V (CCl_4-treated group): Rats were injected with CCl_4 (i.p.) at the dose 0.5 ml/kg b.w. (50 % CCl_4 in olive oil) twice a week for 28 days[30]. Group VI (CYP-treated group): Rats received CYP (i.p) at 40 mg/kg b.w. twice a week for 15 days[31]. Group VII (Irradiated group): Rats were exposed to single dose of 7 Gy delivered at the dose rate of 1.167 Rad / Sec. at Middle Eastern Regional Radioisotope Centre for the Arab Countries, Dokki, Egypt using Cobalt 60 (Co^{60})[32].

Testicular protein extraction

All the animals were anaesthetized and killed by decapitation. Testes were quickly dissected and carefully cleaned of superficial fatty layer, weighed and then washed in ice-cold saline. As mentioned in Elshawi *et al.*[33], the testes were freezed with liquid nitrogen and homogenized in 1 ml water-soluble extraction buffer. The homogenates left in refrigerator

overnight and vortexed for 15 seconds then centrifuged at 10,000 rpm at 4˚C for 15 min. The supernatants containing water-soluble proteins were transferred to new eppendorf tubes and kept at deep-freeze until the different electrophoretic patterns.

Protein Determination

All samples of each group were pooled together and used as one sample. Protein concentration was estimated in the tissue homogenates according to the method suggested by Bradford[34] using bovine serum albumin as standard. The protein concentration in each well should be in the range between 60-80 µg protein.

Electrophoretic protein pattern

To determine the relative molecular weight of isolated proteins, vertical slab, non-denaturing 10 % polyacrylamide gel electrophoresis of samples was carried out according to method suggested by Laemmli[35] using Mini-gel electrophoresis (BioRad, USA), with the modification that samples, gels and running buffers were lacking SDS. The gels contained Acrylamide/Bis (30% T, 2.67% C) (Acrylamide: bis-acrylamide = 29.2:0.8) and 10% glycerol. Equal quantities of protein were loaded in each well. The gel

was run in buffer containing Tris (24 mM) and glycine (194 mM) at room temperature. After completing the electrophoretic run, protein bands were visualized by staining with Coomassie Brilliant Blue G-250 and

destained overnight with 7% (v/v) glacial acetic acid after documentation[36]. The molecular weight of the separated proteins was estimated in comparison to marker of standard molecular weights with regularly spaced bands ranging from 6.458 to 195.755 KDa. 5µl of the marker

loaded in the first well with the samples each run. The native gels were also stained for lipid with Sudan Black B (SBB)[37]. Relative mobilities (Rf) and band percent (B %) of protein and lipoprotein bands were determined.

Electrophoretic localization of in-gel enzyme activity

The native gel was stained for catalase (CAT) pattern according to method described by Siciliano and Shaw[38]. It was stained for peroxidase (Gpx) pattern using benzidine stain prepared according to method of Rescigno *et al*.[39]. The native gel was processed for localization of in-gel esterases (EST) pattern according to method suggested by Ahmad *et al*.[40] who reported that the gel was incubated in reaction mixture containing α, β-naphthyl acetate (5.58 X 10^{-3} mM, pH 7.5) as substrates along with dye coupler Fast Blue RR at 25°C in dark. After developing the dark brown bands of EST activity, the reaction was stopped by fixing the gels in 7% glacial acetic acid for 30 min, followed by preserving the gel in 5% acetic acid prepared in 10% methanol.

Computational Methods

Protein Structure Prediction

Prediction of protein structure is considered as one of the most important and advanced technologies used by computational structural biology and theoretical chemistry. It aims to determine the three-dimensional structure of proteins from sequences of their amino acid. By this technology, it was expressed that the tertiary structure of protein predicted from its primary structure.

Comparative Protein Modeling

The solved structures were used as starting points or templates by the comparative protein modeling. This technology is effective because it shows that there is a limited set of tertiary structural motifs to which most proteins belong although number of actual proteins is vast. Furthermore, it was suggested that there are only around 2000 distinct protein folds in nature, though there are many millions of different proteins. Sequence-based methods for identifying protein homology compare sequences to find similarities that are unlikely to occur by chance. Essentially all methods employ some sort of scheme to judge amino acid substitutions, insertions and deletions. Based on the scoring scheme a query sequence is aligned to another sequence or to a profile that represents a set of sequences. In an alignment equivalent amino acids are set side-by-side so that insertions and deletions become apparent as shown in Fig. 1. The score of the sequence, which is used to detect homology, is directly related to the alignment. Profile-profile sequence-based homology detection was used. Sequences can be scored globally or locally. In the former case, the alignment is over the entire length of the sequences. From a biological point of view this is not always desired because related proteins may not have recognizable homology along their entire length. Proteins may share only one out of several domains. Local scoring aligns subsequences only and can be better for finding local similarities. It is also possible to align a global domain model locally to a sequence, (global/local scoring) or to align part of a domain model locally to a sequence (local/local scoring). Based on the amount of information built into the scoring scheme, existing methods for sequence-based homology detection can broadly be divided into three categories. pair-wise methods that compare sequences one by one, profile methods that compare one sequence to a family of sequences and profile-profile methods that compare families of sequence. It has been shown that at comparable levels of misclassifications, profile based methods are more sensitive than pair-wise methods[41,42] and that profile-profile methods are even more sensitive[43]. All the modeling methods belong to one of the following groups: Homology modeling depends on the reasonable assumption that the two homologous proteins will involve in very similar structures. Due to a protein's fold is more evolutionarily conserved than sequence of its amino acids, comparative modeling of a target sequence can be carried out with reasonable accuracy on a very distantly related template. This provided with evidence that there is relationship between target and template discerned through alignment of the sequence. Based on study of the comparative modeling, it was suggested that the primary bottleneck arises from difficulties in alignment rather than from errors in prediction of structure given a known-good alignment[44]. When the target and template have identical sequences, the homology modeling becomes the most accurate unsurprisingly. Protein threading is used for scanning sequence of the amino acid in an unknown structure against solved structures in a database[45]. Assessment of compatibility of the sequence to the structure in each case is carried out by a scoring function, thus yielding possible three-dimensional models. Also, this type of the technological method is known as 3D-1D fold recognition due to its compatibility analysis between three-dimensional structures and sequences of linear protein. Moreover, this method has given rise to methods performing an inverse folding search through evaluating compatibility of a given structure with a large sequences in database, thus it is possible to predict which sequences have the potential to produce a given fold[46,47].

Molecular Dynamic Simulations

Concepts of the molecular dynamic simulations are quite simple. In these simulations, it is possible to follow the trajectories of N particles interacting via a many-body potential U (r_1, r_2, …, r_N) using Newton's equation of motion[48]:

$$m_i \frac{d^2 r_i}{dr^2} = -\nabla_i U(r_1, ..., r_N) \;\; ; \;\; i = 1, ..., N$$

Where m_i and r_i indicate the mass and position of the particle. On the other hand, the force on it is given by the potential gradient U. Otherwise, in Brownian dynamic simulations, only the ions are simulated explicitly, all the atoms (ions, water, protein and lipid) can be included in the molecular dynamics. At every time step, the potential function is recalculated using new positions of the particles to determine their positions a short time later, and this process is iterated for a large number of steps until a statistically satisfactory data set is generated. The success of molecular dynamics simulations in capturing the

dynamics of the real system hinges critically on how accurately the potential functions or force fields are selected. In the past two decades, numerous studies have been carried out to develop force fields for biomolecular applications, and these are incorporated into several user-friendly computer programs for simulation of biomolecular systems[49,50]. In these programs, the non-bonded interactions between atoms are represented by Coulomb and Lennard-Jones potentials. Pairwise interactions are used for all the atoms in the system, and the potential parameters are
determined empirically from spectroscopic data and fits to bulk properties. Most atoms in the system are also covalently bonded to other atoms, and these bonds are represented in molecular dynamics by a set of force parameters. For a geometry in Fig. 2 the bonds will typically involve the separation $r_{12} = |r_1 - r_2|$ between adjacent pairs of atoms in a molecular framework. The bend angles θ_{123} is between successive bond vectors (r2 − r1) and (r2 − r3). Usually this bending term is taken to be quadratic in the angular displacement from the equilibrium value. The torsion angles Φ_{1234} are defined in terms of three connected bonds, hence four atomic coordinates:

$$\cos\phi_{1234} = -\hat{n}_{123} \cdot \hat{n}_{234}$$

Where $n_{123} = r_{12} \times r_{23}$, $n_{234} = r_{23} \times r_{34}$.
The normal unit defined by each pair of bonds. Usually the torsional potential involves an expansion in periodic functions[51].

RESULTS

Electrophoretic protein pattern in the testicular tissue of healthy rats produced 15 bands with Rfs ranged between 0.10 - 0.98 (Mwts 6.70 - 216.96 KDa and B % 0.39 - 16.70). There was only one common bands noticed with Rf 0.98 (Mwt 6.70 KDa and B % 1.96). There was only one characteristic band appeared in irradiated group with Rf 0.64 (Mwt 17.85 KDa and B % 10.07). As compared to control, the 1st normal band (Rf 0.10, Mwt 216.96 KDa and B % 16.70) disappeared from CCl_4-treated and irradiated groups. The 3rd normal band (Rf 0.27, Mwt 93.75 KDa and B % 3.82) disappeared from CYP-treated group. The 4th band (Rf 0.33, Mwt 58.49 KDa and B % 1.36) disappeared from Pb_2COOH-treated and Li_2CO_3-treated groups. The 6th band (Rf 0.45, Mwt 29.85 KDa and B % 6.78) disappeared from irradiated group. Several normal bands (Rfs 0.49, 0.79, 0.84, 0.87 and 0.91, Mwts 26.29, 14.36, 12.81, 11.38 and 9.96 KDa and B % values 7.64, 5.10, 3.73, 3.33 and 10.08) disappeared from CYP-treated group. As shown in Table 1 and illustrated in Fig. 3a, Pb_2COOH caused quantitative mutation represented by decreasing B % of the 1st, 5th, 8th and 14th bands (Rfs 0.11, 0.42, 0.55 and 0.92, Mwts 205.15, 34.04, 21.61 and 9.25 KDa and B % 8.94, 3.00, 0.63 and 6.68 respectively) and by increasing B % of the 11th band (Rf 0.80, Mwt 14.16 KDa and B % 38.85). Li_2CO_3 administration caused disappearance of 2 normal bands with appearance of 2 abnormal bands with Rfs 0.14 and 0.53 (Mwts 187.26 and 23.13 KDa and B % 8.44 and 2.39) respectively. It was

PTSX--------PQTQG----LAKD-------AWEIPRESL

PT + PQ+ GL + AE + S

PTRRTFLDPQSCGDLLQAVHLFAKELDAKSV

Figure 1: An alignment between two sequences. Conserved amino acids are aligned and insertions are marked with dashes.

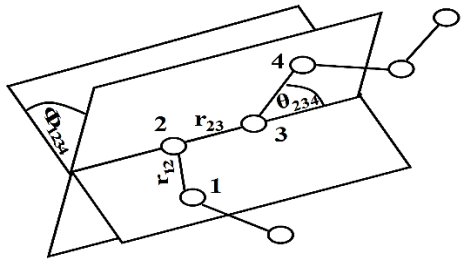

Figure 2: Geometry of a simple chain molecule, illustrating the definition of interatomic distance r_{23}, bend angle θ_{234}, and torsion angle Φ_{1234}.

probable that the 2nd band was deviated to be appeared with Rf 0.23 (Mwt 120.81 KDa and B % 3.76). This was in association with the quantitative mutation represented by decreasing B % of the 1st, 4th, 7th and 12th bands (Rfs 0.10, 0.33, 0.50 and 0.85, Mwts 215.78, 55.78, 25.29 and 12.27 KDa and B % values 9.62, 0.31, 0.53 and 8.64 respectively)
and by increasing B % of the 3rd, 6th and 9th bands (Rfs 0.28, 0.45 and 0.68, Mwts 87.32, 30.40 and 16.78 KDa and B % 5.30, 14.33 and 30.03 respectively). From the SI values, the lowest SI value (0.42) was recorded with CYP-treated group and the highest SI value (0.79) was recorded with Pb_2COOH-treated group (Fig. 3b). Lipoprotein pattern in healthy testicular tissue produced 5 bands with Rfs 0.05, 0.14, 0.26, 0.38 and 0.85 (B % 6.07, 19.62, 29.75, 12.60 and 31.97) respectively. There was one common band appeared with Rf 0.05 (B % 6.07) (Table 2 and illustrated in Fig. 4a). As compared to control, CYP administration and irradiation caused disappearance of the 5th normal band. Pb_2COOH administration caused qualitative alterations represented by disappearanc of the 2nd band with deviation of the 3rd and 4th bands to be appeared with Rfs 0.28 and 0.44 (B % 14.01 and 41.10). Li_2CO_3 administration caused qualitative alterations represented by disappearance of 2 normal bands with appearance of one abnormal band (Rf 0.07, B % 22.88). In the DXR-treated group, the qualitative alterations were represented by disappearance of 2 normal bands with deviation of the 3rd normal band to be appeared with Rf 0.25 (B % 47.00). This was in addition to the quantitative mutation which was represented by increasing B % of the 1st band (Rf 0.04, B % 21.45). In the CCl_4-treated group, the qualitative alterations were represented by disappearance of one normal bands with appearance of one abnormal band with Rf 0.06 (B % 7.33). This was in addition to the quantitative mutation which was

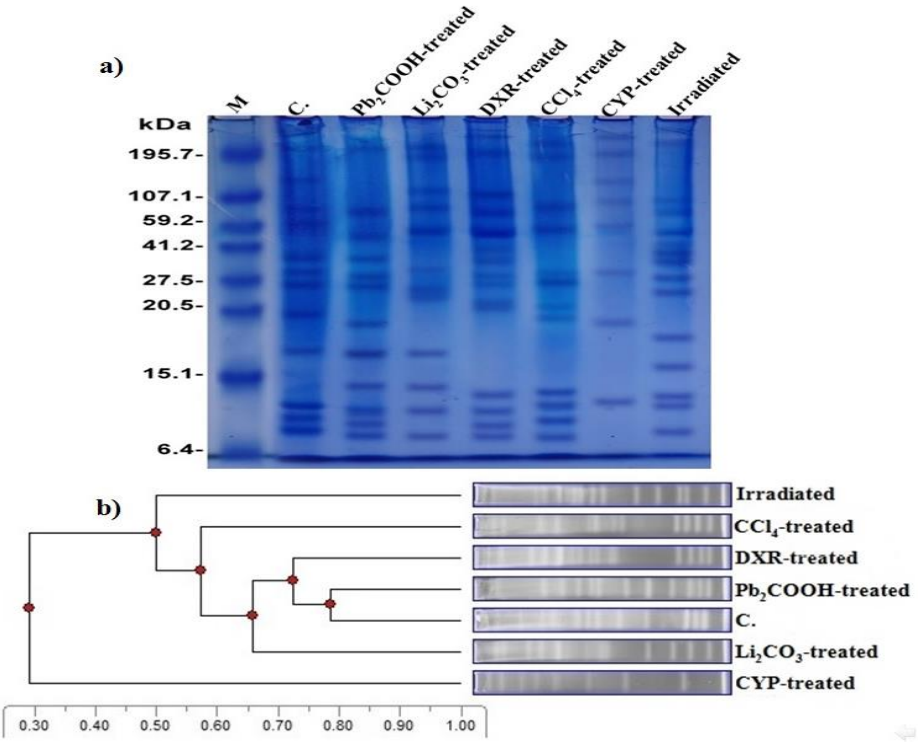

Figure 3: (a) Electrophoretic protein pattern showing toxic effect of Pb_2COOH, Li_2CO_3, DXR, CCl_4, CYP and irradiation on protein pattern in testicular tissue of male rats, (b) Dendogram showing the similarity and relatiohship among Pb_2COOH-treated, Li_2CO_3-treated, DXR-treated, CCl_4-treated, CYP-treated and Irradiated groups in male rats as compared to control.

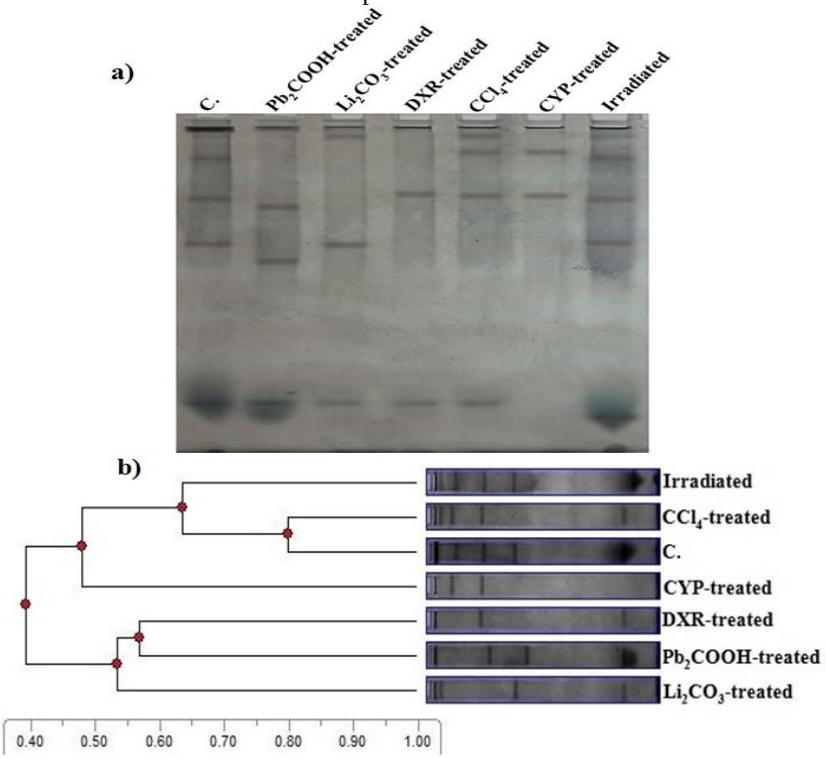

Figure 4: (a) Electrophoretic lipoprotein pattern showing toxic effect of Pb_2COOH, Li_2CO_3, DXR, CCl_4, CYP and irradiation on lipoprotein pattern in testicular tissue of male rats, (b) Dendogram showing the similarity and relatiohship among Pb_2COOH-treated, Li_2CO_3-treated, DXR-treated, CCl_4-treated, CYP-treated and Irradiated groups in male rats as compared to control.

represented by increasing B % of the 3rd band (Rf 0.26, B % 48.22). In the CYP-treated group, the qualitative alterations were represented by disappearance of 2 normal bands with deviation of the 3rd normal band to be appeared

with Rf 0.24 (B % 52.36). The quantitative mutation was represented by increasing B % of the 2nd band (Rf 0.12, B % 41.47). In the irradiated group, the qualitative alterations were represented by appearance of one abnormal band (Rf

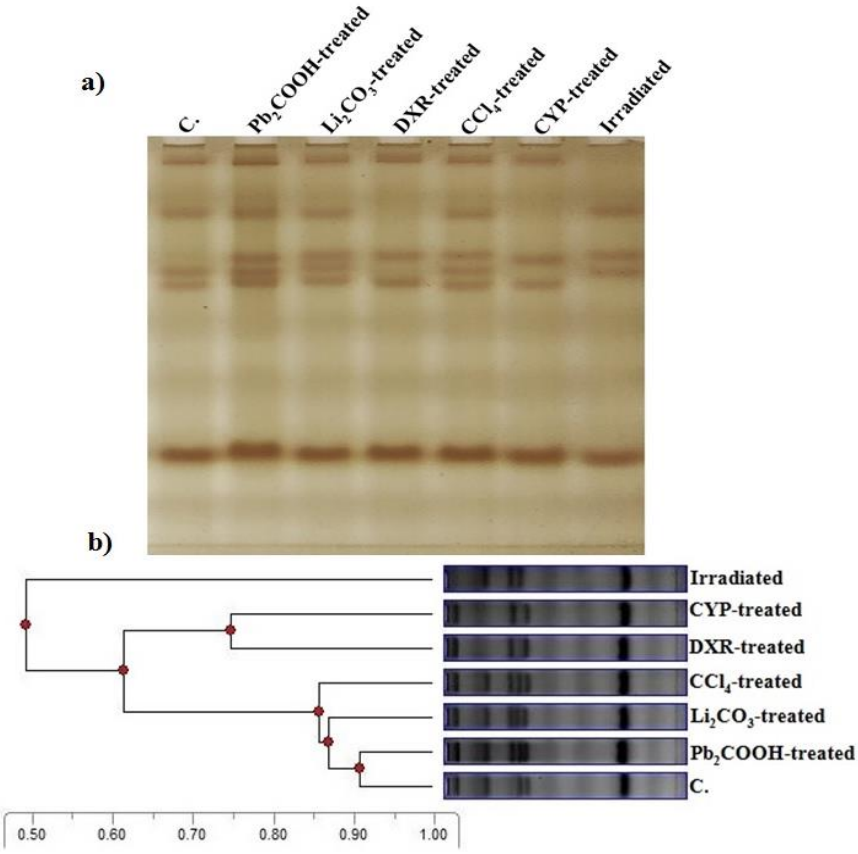

Figure 5: (a) Electrophoretic CAT pattern showing toxic effect of Pb_2COOH, Li_2CO_3, DXR, CCl_4, CYP and irradiation on CAT pattern in testicular tissue of male rats, (b) Dendogram showing the similarity and relatiohship among Pb_2COOH-treated, Li_2CO_3-treated, DXR-treated, CCl_4-treated, CYP-treated and Irradiated groups in male rats as compared to control.

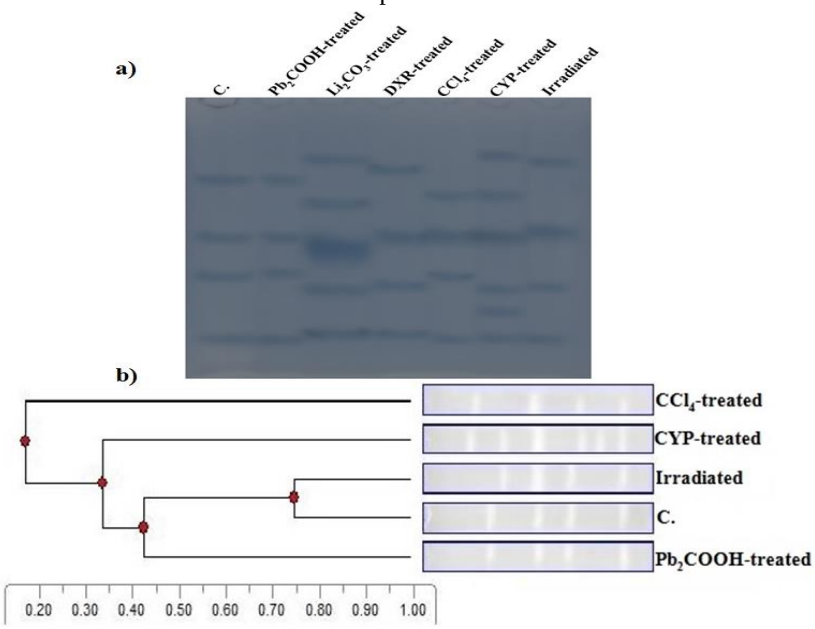

Figure 6: (a) Electrophoretic Gpx pattern showing toxic effect of Pb_2COOH, Li_2CO_3, DXR, CCl_4, CYP and irradiation on Gpx pattern in testicular tissue of male rats, (b) Dendogram showing the similarity and relatiohship among Pb_2COOH-treated, Li_2CO_3-treated, DXR-treated, CCl_4-treated, CYP-treated and Irradiated groups in male rats as compared to control.

0.07, B % 4.65) with deviation of the 5th normal band to be appeared with Rf 0.90 (B % 32.28). There was no quantitative mutation. The lowest SI value (0.44) was observed with Pb_2COOH-treated group and the highest SI values (0.73 and 0.80) were observed with CCl_4-treated and irradiated groups (Fig. 4b). There was complete similarity between DXR-treated and CYP-treated groups in number and arrangement of the bands. As revealed in Table 3 and illustrated in Fig. 5a, 5 types of CAT enzyme were produced in healthy testicular tissue with Rfs 0.07, 0.19, 0.31, 0.35 and 0.75 (B % values 14.31, 25.65, 15.14, 22.13 and 22.78). There was only one common band appeared with Rf 0.75 (B % 22.78). As compared to control group, Pb_2COOH administration caused obvious qualitative alterations represented by existence of one abnormal band with Rf 0.28 (B % 10.22). Irradiation caused disappearance of the 1st and 4th normal types of the enzyme. Li_2CO_3 caused qualitative alterations represented by appearance of one abnormal type with Rf 0.27 (B % 9.74). This was in addition to the quantitative mutation occurred by decreasing B % in the band appeared with Rf 0.33 (B % 9.85). In all treated groups, there was one abnormal band appeared with different data. This band was appeared with Rf 0.28 (B % 16.19) in DXR-treated group, with Rf 0.28 (B % 8.39) in CCl_4-treated group, with Rf 0.29 (B % 13.11) in CYP-treated group and with Rf 0.28 (B % 13.01) in irradiated group. On the other hand, there was quantitative mutation occurred through increasing B % severely in the 1st type of the enzyme appeared in the DXR-treated group (Rf 0.06 and B % 47.65) and CYP-treated group (Rf 0.05 and B % 43.20). The lowest SI value (0.69) was noticed in DXR-treated, CYP-treated and irradiated groups. There was complete similarity between the Li_2CO_3-treated and irradiated groups (Fig. 5b). The highest SI value (0.91) was observed with Pb_2COOH, Li_2CO_3-treated and CCl_4-treated groups. Four types of Gpx enzyme were produced in healthy testicular tissue with Rfs 0.30, 0.51, 0.66 and 0.88 (B % values 29.11, 19.44, 32.41 and 19.04) respectively. There were no common bands. As shown in Table 4 and illustrated in Fig. 6a, it was found that Pb_2COOH administration caused qualitative alterations represented by disappearance of the 4th type with deviation of the 3rd type to be appeared with Rf 0.64 (B % 41.28). Li_2CO_3 administration caused qualitative abnormalities represented by disappearance of the 1st, 2nd and 3th types with deviation of the 4th type to be appeared with Rf 0.86 (B % 19.75). In addition, there were 4 abnormal bands appeared with Rfs 0.23, 0.39, 0.55 and 0.70 (B % values 21.18, 19.17, 1.41 and 38.49) respectively. The abnormalities occurred with the same degree in DXR-

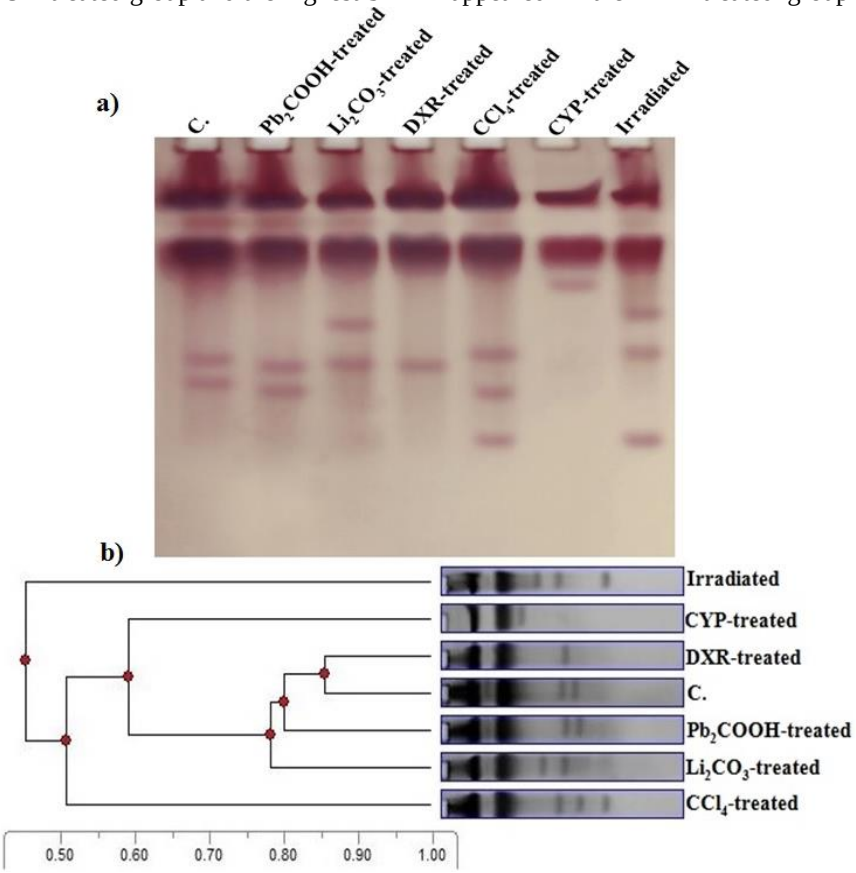

Figure 7: (a) Electrophoretic EST pattern showing toxic effect of Pb_2COOH, Li_2CO_3, DXR, CCl_4, CYP and irradiation on EST pattern in testicular tissue of male rats, (b) Dendogram showing the similarity and relatiohship among Pb_2COOH-treated, Li_2CO_3-treated, DXR-treated, CCl_4-treated, CYP-treated and Irradiated groups in male rats as compared to control.

treated and irradiated groups. These alterations were represented by disappearance of the 1st type of the enzyme and appearance of one abnormal band with deviation of the other types of enzyme to be appeared with different data. In the DXR-treated group, the abnormal band was appeared with Rf 0.26 (B % 33.12). The 2nd, 3rd and 4th types deviated to be appeared with Rfs 0.52 and 0.68 (B % values 23.19 and 23.54). While in irradiated group, the abnormal band appeared with Rf 0.23 (B % 33.28). The normal types were deviated to be appeared with Rfs 0.49 and 0.69 (B % 0.58 and 49.70). In CCl_4-treated group, the qualitative alteration was represented by disappearance of the 1st type with appearance of one abnormal band (Rf 0.36, B % 22.48). The quantitative mutation occurred by decreasing B % of the 2nd type (Rf 0.51 and B % 0.89) and increasing B % of the 3rd type (Rf 0.65 and B % 56.37). The lowest SI value (0.25) was noted with irradiated group and the hightest value (0.75) was observed with CCl_4-treated group. In the Li_2CO_3-treated and DXR-treated groups, it was observed that all the bands were not matched with all bands of the other groups (Fig. 6b). Four types of EST enzyme were produced in testicular tissue of control rats

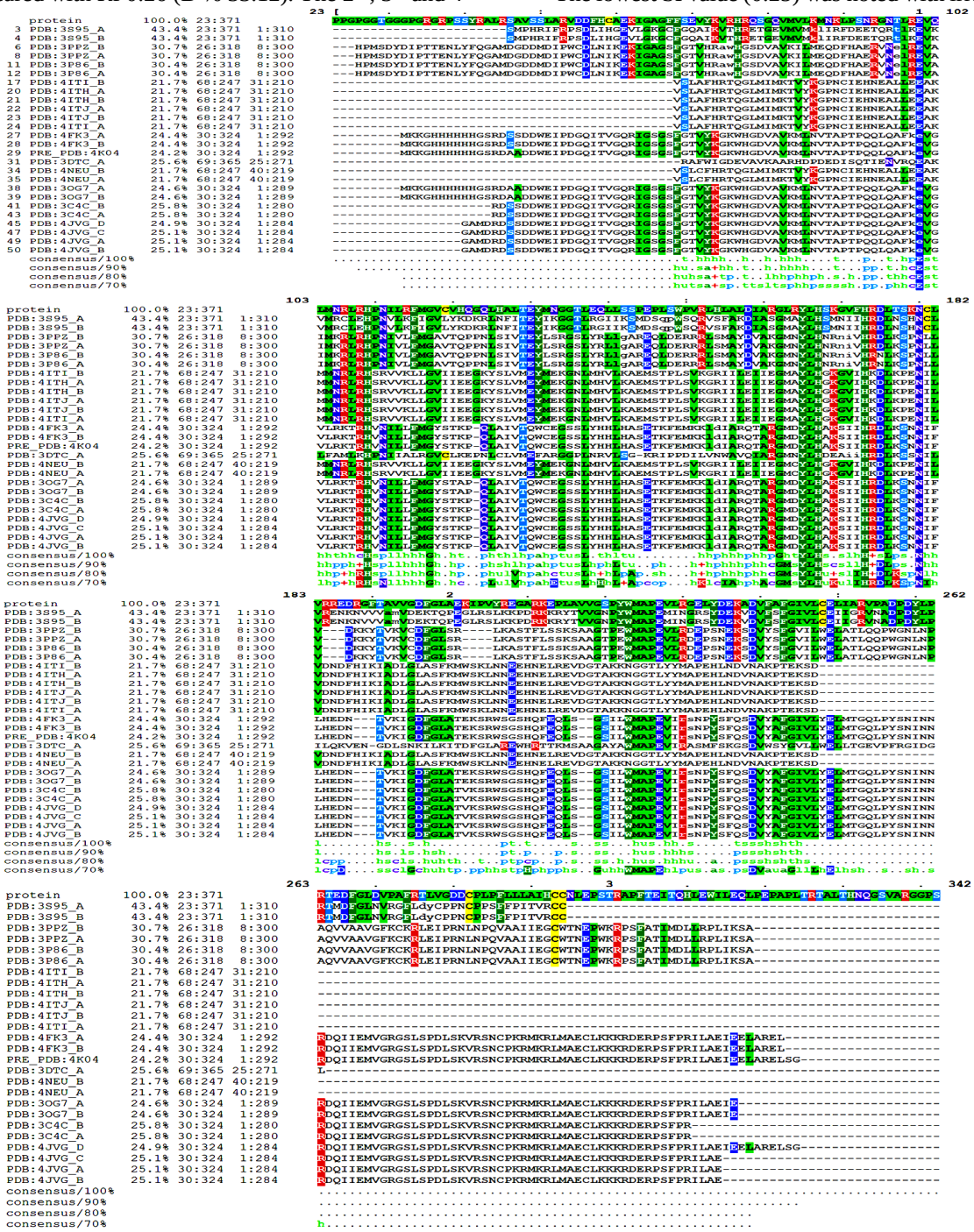

Figure 8: Sequence alignments of TESK1 protein kinases and its homolog structures extracted from the protein data bank (PDB) database. Amino acids are colored based on their properties.

with Rfs 0.14, 0.26, 0.50 and 0.57 (B % values 38.78, 33.44, 8.12 and 19.66) respectively (Table 5 and illustrated in Fig. 7a). There were 2 common bands appeared with Rfs 0.14 and 0.26 (B % 38.78 and 33.44). Administration of Pb_2COOH caused no obvious qualitative or quantitative mutations as compared to control sample. Li_2CO_3 administration caused qualitative mutation represented by disappearance of the 4th normal type with appearance of one abnormal band with Rf 0.42 (B % 9.90). This was in addition to increasing B % of the 3rd normal band (Rf 0.52 and B % 29.28). In the DXR-treated group, the alterations were represented by disappearance of the 4th type with increasing B % of the 3rd type (Rf 0.51 and B % 23.86). In the CCl_4-treated group, the alterations occurred qualitatively by appearance of one abnormal band (Rf 0.69 and B % 7.79) without disappearance of the normal types of enzymes. In the CYP-treated group, the alterations occurred qualitatively by disappearance of the 3rd and 4th types of enzyme with appearance of one abnormal band (Rf 0.33 and B % 19.70). In the irradiated group, the qualitative alterations occurred through disappearance of the 4th type of enzyme with appearance of 2 abnormal bands with Rf 0.40 and 0.68 (B % 8.51 and 8.14) respectively. There was complete similarity between Pb_2COOH-treated and Li_2CO_3-treated groups (equal SI values 0.75). The lowest SI value (0.44) was observed with irradiated group. The highest SI value (0.86) was noticed with DXR-treated group (Fig. 7b). Although the genome expression of TESK1 protein as well as its one dimension sequence were identified previously [Jiro Toshima, Tomoko Tanaka, Kensaku Mizuno, THE JOURNAL OF BIOLOGICAL CHEMISTRY, 274, 12171-12176 (1999) - S. Davila, F. E. Froeling, A. Tan, C. Bonnard, G. J. Boland, H. Snippe, M. L. Hibberd, M. Seielstad, Genes Immun. 11, 232-238 (2010)], however its crystal structure is not known yet. Structural data has vital role not only in comparative analysis between TESK1 and other kinase protein but also for structural activity relationship (SAR) investigation. During the current work, it was noted that model of the TESK1 was quite big and no available template for the whole sequence and its first half (up to residue 333) was synthesized with a very good homology model. For the rest of the model (334 - 626), a draft structure was carried out using residue addition algorithm but its 3D structure is not good. The current framework concerns to obtain 3D model of TESK1 using homology and threading techniques. The 3D model was built by means of restraint-based comparative modeling. Sequence identity percentages between the target TESK1 and templates obtained from FASTA and BLAST databases [H. McWilliam H, W. Li, M. Uludag, S. Squizzato, Y. M. Park, N. Buso, A. P. Cowley, R. Lopez, Analysis Tool Web Services from the EMBL-EBI, Nucleic acids research 41 (Web Server issue) :W597-600 (2013 Jul) - A. Morgulis, G. Coulouris, Y. Raytselis, T. L. Madden, R. Agarwala, A. A. Schäffer, "Database indexing for production MegaBLAST searches." Bioinformatics 15: 1757-1764 (2008)]. Templates were selected according to the similarity with the query sequence (with similarity percent of 43.0 ± 2%). The model was construct using multiple alignment by means of restraint-based comparative modeling, using the X-ray crystallographic structures of human LIMK1 kinase (PDB ID: 3s95), Tank-binding kinase I (PDB ID: 4iw0), tyrosine-protein kinase (PDB: 2fo0), and G protein coupled receptor kinases (PDB ID: 3c4w, 2acx and 3NYN) as templates. Finally the hydrogen atoms were added. [Y. Zhang. I-TASSER server for protein 3D structure prediction. BMC Bioinformatics, 9:40 (2008) - A. Roy, A. Kucukural, Y. Zhang. I-TASSER: a unified platform for automated protein structure and function prediction. Nature Protocols, vol 5, 725-738 (2010) - A. Roy, J. Yang, Y. Zhang. COFACTOR: an accurate comparative algorithm for structure-based protein function annotation. Nucleic Acids Research, vol 40, W471-W477 (2012)]. Fig. 9 shows the constructed 3D model of TESK1 model where high similarity domains (from residue 23 to residue 341) were constructed by threading and the other domains (1~23 and 341~626) were

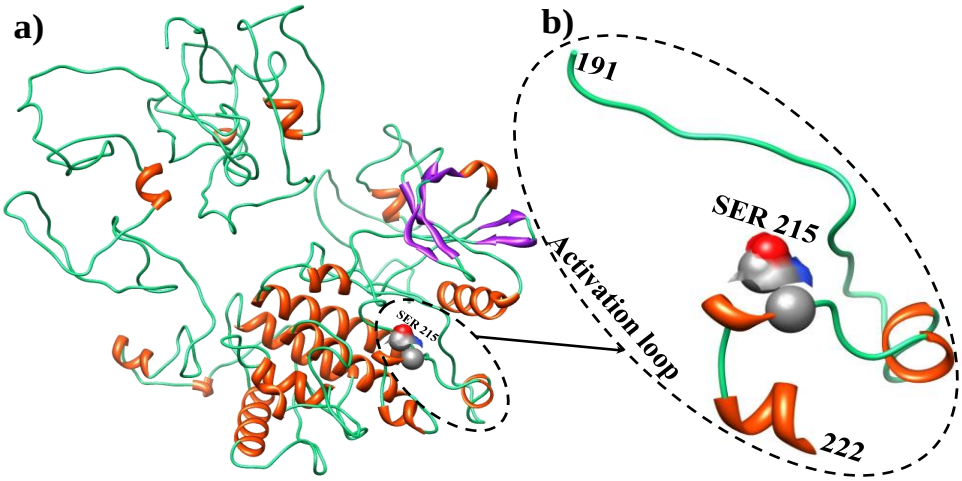

Figure 9: 3D-Homology model of TESK1 predicted by I-TASSER platform, a) The full length protein structure and b) the activation loop subdomain. Residues are colored based on the secondary structure (helix in orange, strand in purple and coil loop in cyan).

constructed through insertion algorithms. The activation loop (191~222) has flexible coil shape attached to short helix at the end. This subdomain consists of the SER215 that is known to be phosphorylated within kinase activation loop reaction [Jiro Toshima, Tomoko Tanaka, Kensaku Mizuno, The Journal of Biological Chemistry, 274 : 12171-12176 (1999)].

DISCUSSION

The difference in protein pattern acts as a tool to identify the physiological state of the testicular tissue in the treated groups as compared to control. It was reported that electrophoresis used to detect the mutations reflected as quantitative changes in the protein expression[52]. The SI value is inversely proportional to the genetic distance. When the SI value between the control and all the treated groups recorded low values, this indicates to toxic effect of these substances and the differences in number and arrangement of the protein bands[53,54]. The alterations in protein pattern can be detected electrophoretically due to the chemical changes which may be represented by fragmentation, cross-linking, aggregation and oxidation by oxygen radicals. These disturbances lead to variation of the different biological processes due to activation of the genes which are responsible for synthesis of different types of proteins not produced in the healthy group[55]. During the present study, all the toxic factors exhibited different mutagenic effects and caused irreversible changes at the molecular level. The protein bands in testicular tissue of treated rats may differ qualitatively through disappearance in some normal bands or appearance of new abnormal ones. Disappearance of the normal bands in treated rats may be attributed to effects of toxic substances which inhibit expression of the genes responsible for synthesis of these deleted proteins. In addition, the alterations may occur quantitatively through remaining the bands but with different quantity. This may be explained by effect of the toxic substances which could not inhibit expression of the genes which are responsible for synthesis of this protein type, but it may be affected only at the quantitative level. The quantitative mutation may occur due to disturbances in the golgi apparatus which subsequently leads to accumulation of protein due to impairment of glycosylation and glycoprotein trafficking[56]. During the present study, lithium caused alterations in the protein pattern. This was in accordance with Mathur *et al*.[57] who reported that the toxicity may occur due to presence of the reactive oxygen species (ROS). These radicals prevent the spin restriction of O_2 giving rise to generation of ROS and chain reaction. This leads to structural alterations in the native the proteins. The abnormalities in the different electrophoretic patterns as a result of lithium exposure may refer to elevation of lipid peroxidation reaction[58]. During another recent point of view, it was suggested that the disturbances occurred as a result of lithium administration may not be caused due to the oxidative stress or lipid peroxidation. The toxicity may occur as a result of other possible

Table 1: Electrophoretic pattern showing effect of Pb_2COOH, Li_2CO_3, DXR, CCl_4, CYP and irradiation on protein pattern in testicular tissue of male rats.

Control			Toxic substances															
			Pb_2COOH-treated			Li_2CO_3-treated			DXR-treated			CCl_4-treated			CYP-treated			Irradiated		
Rf.	Mwt	B. %	Rf.	Mwt	B. %	Rf.	Mwt	B. %	Rf.	Mwt	B. %	Rf.	Mwt	B. %	Rf.	Mwt	B. %	Rf.	Mwt	B. %
0.10	216.96	16.70	0.10	216.96	25.60	0.10	215.78	9.62	0.06	245.32	8.04	0.09	221.69	8.58	0.06	245.32	4.78	0.08	229.96	5.65
0.19	146.54	6.54	0.28	84.20	0.69	0.14	187.26	8.44	0.11	205.15	8.94	0.13	194.49	11.86	0.12	200.43	5.81	0.25	108.23	16.78
0.27	93.75	3.82	0.35	49.39	5.82	0.23	120.81	3.76	0.24	115.06	3.33	0.27	88.38	5.36	0.20	142.99	13.54	0.29	80.13	5.27
0.33	58.49	1.36	0.41	35.85	5.56	0.28	87.32	5.30	0.28	83.17	3.86	0.35	51.55	1.51	0.25	107.10	8.11	0.34	53.89	0.36
0.41	36.12	7.03	0.46	29.14	7.37	0.33	55.78	0.31	0.35	48.88	3.59	0.44	30.98	13.16	0.33	55.78	15.76	0.38	41.93	4.62
0.45	29.85	6.78	0.49	25.85	0.53	0.45	30.40	14.33	0.39	40.14	0.40	0.49	25.85	7.37	0.60	19.16	29.98	0.40	38.50	0.25
0.49	26.29	7.64	0.60	19.23	19.18	0.50	25.29	0.53	0.42	34.04	3.00	0.56	21.31	3.53	0.83	13.21	19.69	0.43	32.87	6.16
0.57	20.59	0.39	0.68	16.88	0.54	0.53	23.13	2.39	0.46	28.97	6.16	0.58	19.79	26.15	0.98	6.84	2.33	0.47	27.66	3.94
0.68	16.88	11.46	0.78	14.72	18.37	0.68	16.78	30.03	0.49	26.14	6.22	0.80	14.06	4.07	0.98	6.84	0.00	0.52	24.10	14.89
0.74	15.58	14.09	0.85	12.33	4.11	0.78	14.59	8.01	0.55	21.61	0.63	0.83	12.98	4.81	—	—	—	0.64	17.85	10.07
0.79	14.36	5.10	0.89	10.91	3.53	0.85	12.27	8.64	0.80	14.16	38.85	0.88	11.25	5.44	—	—	—	0.73	15.85	8.98
0.84	12.81	3.73	0.92	9.46	7.26	0.92	9.25	7.05	0.85	12.20	4.67	0.94	8.68	6.07	—	—	—	0.79	14.31	1.22
0.87	11.38	3.33	0.99	6.47	1.44	0.98	6.70	1.58	0.89	10.85	3.73	0.98	6.84	2.09	—	—	—	0.83	12.98	11.69
0.91	9.96	10.08	—	—	—	—	—	—	0.92	9.25	6.68	—	—	—	—	—	—	0.91	10.03	7.47
0.98	6.70	1.96	—	—	—	—	—	—	0.98	6.70	1.90	—	—	—	—	—	—	0.98	6.77	2.65

Rf.: Relative Mobility, Mwt.: Molecular Weight, B. %: Band Percent.
In each lane, arrangement of the bands is not correlated to arrangement of the bands in the other lanes.

mechanism due to lithium toxicity[59]. In the current experiment, administration of CCl_4 induced testis toxicity through by altering the protein pattern. This was in agreement with Terzi *et al.*[60] who postulated that CCl_4 caused generation of the ROS leading to loss of germ cells, inhibition of structural deterioration of the sertoli cells in seminiferous tubules of testicular tissue in rat[61]. DXR administration induced testicular toxicity. This was in accordance with Patil and Balaraman[62] who reported that DXR induced a significant decline in testes weight, sperm count, serum testosterone, increase in serum lactate dehydrogenase and increases lipid peroxidation in that tissue. The injury in this organ may occur due the oxidative stress induced by the reactive intermediates semiquinone formed from DXR. The semiquinone radical intermediates react with molecular oxygen to form ROS that interact with cellular macromolecules causing cytological damage[63]. Irradiation caused differences in protein pattern. This was in agreement with Moon and Song[64] who suggested that irradiation caused initial fragmentation of polypeptide chains and leads to lowering the ordered protein structure as a result of subsequent aggregation and degeneration of proteins. The alterations in protein pattern may occur as a result of the DNA damage after irradiation, resulting in subsegment changes in mRNA. Subsequently, this leads to impairment in transcription of the genes and hence inhibition of protein synthesis[65].

Table 2: Electrophoretic pattern showing effect of Pb_2COOH, Li_2CO_3, DXR, CCl_4, CYP and irradiation on lipoprotein pattern in testicular tissue of male rats.

Control		Toxic substances											
		Pb_2COOH-treated		Li_2CO_3-treated		DXR-treated		CCl_4-treated		CYP-treated		Irradiated	
Rf.	B. %	Rf.	B. %	Rf.	B. %	Rf.	B. %	Rf.	B. %	Rf.	B. %	Rf.	B. %
0.05	6.07	0.04	10.25	0.04	9.55	0.04	21.45	0.04	3.37	0.04	6.17	0.04	2.70
0.14	19.62	0.28	14.01	0.07	22.88	0.25	47.00	0.06	7.33	0.12	41.47	0.07	4.65
0.26	29.75	0.44	41.10	0.39	38.40	0.86	31.56	0.12	12.66	0.24	52.36	0.13	20.11
0.38	12.60	0.85	34.64	0.86	29.17	—	—	0.26	48.22	—	—	0.26	20.66
0.85	31.97	—	—	—	—	—	—	0.86	28.42	—	—	0.38	19.59
—	—	—	—	—	—	—	—	—	—	—	—	0.90	32.28

Rf.: Relative Mobility, B.%: Band Percent.
In each lane, arrangement of the bands is not correlated to arrangement of the bands in the other lanes.

Table 3: Electrophoretic pattern showing effect of Pb_2COOH, Li_2CO_3, DXR, CCl_4, CYP and irradiation on CAT pattern in testicular tissue of male rats.

Control		Toxic substances											
		Pb_2COOH-treated		Li_2CO_3-treated		DXR-treated		CCl_4-treated		CYP-treated		Irradiated	
Rf.	B. %	Rf.	B. %	Rf.	B. %	Rf.	B. %	Rf.	B. %	Rf.	B. %	Rf.	B. %
0.07	14.31	0.07	15.35	0.06	21.60	0.06	47.65	0.06	17.98	0.05	43.20	0.17	55.44
0.19	25.65	0.19	24.45	0.18	26.05	0.28	16.19	0.19	23.35	0.29	13.11	0.28	13.01
0.31	15.14	0.28	10.22	0.27	9.74	0.34	10.95	0.28	8.39	0.35	24.17	0.32	12.91
0.35	22.13	0.32	7.49	0.30	6.40	0.76	25.22	0.32	7.47	0.75	19.51	0.76	18.64
0.75	22.78	0.34	21.22	0.33	9.85	—	—	0.35	25.14	—	—	—	—
—	—	0.74	21.27	0.75	26.36	—	—	0.76	17.67	—	—	—	—

Rf.: Relative Mobility, B.%: Band Percent.
In each lane, arrangement of the bands is not correlated to arrangement of the bands in the other lanes.

In addition, the formation of free radicals can cause breakage of chemical bonds and destruction of protein molecules[66]. The testes are susceptible to oxidative stress caused by free radicals. ROS-scavenging enzymes play a vital role in the testicular tissue. The CAT and Gpx are particularly important during the testicular regression[67]. The oxidative stress leads to changes in activities of CAT and Gpx and hence leading to impairment of the spermatogenesis process[68]. During the present work, it was found that irradiation caused alterations in the electrophoretic isoenzymes. This was in accordance with finding of Manciluae *et al.*[69] who reported that irradiation affected activity of the enzymes due to inhibition in synthesis of the DNA and RNA which are responsible for biosynthesis of these enzymes. Moreover, the abnormalities might refer to the lesions induced by radiation and these lesions repair may occur at sites non-specific for synthesis of these enzymes[70]. It is well known that the testes are a comparatively rich source of EST enzyme. The pubertal growth is correlated with the increase of testicular EST in the gonads[71]. So, EST enzyme selected to be under the present study. According to results of the current study, all the toxic factors caused qualitative and quantitative alterations in the electrophoretic EST

Table 4: Electrophoretic pattern showing effect of Pb_2COOH, Li_2CO_3, DXR, CCl_4, CYP and irradiation on Gpx pattern in testicular tissue of male rats.

Control		Toxic substances											
		Pb_2COOH-treated		Li_2CO_3-treated		DXR-treated		CCl_4-treated		CYP-treated		Irradiated	
Rf.	B. %	Rf.	B. %	Rf.	B. %	Rf.	B. %	Rf.	B. %	Rf.	B. %	Rf.	B. %
0.30	29.11	0.30	36.94	0.23	21.18	0.26	33.12	0.36	22.48	0.22	17.93	0.23	33.28
0.51	19.44	0.51	21.78	0.39	19.17	0.52	23.19	0.51	0.89	0.35	18.65	0.49	0.58
0.66	32.41	0.64	41.28	0.55	1.41	0.68	23.54	0.65	56.37	0.51	0.92	0.69	49.70
0.88	19.04	—	—	0.70	38.49	0.86	20.15	0.88	20.26	0.70	33.92	0.88	16.45
—	—	—	—	0.86	19.75	—	—	—	—	0.78	11.47	—	—
—	—	—	—	—	—	—	—	—	—	0.88	17.11	—	—

Table 5: Electrophoretic pattern showing effect of Pb_2COOH, Li_2CO_3, DXR, CCl_4, CYP and irradiation on EST pattern in testicular tissue of male rats.

Control		Toxic substances											
		Pb_2COOH-treated		Li_2CO_3-treated		DXR-treated		CCl_4-treated		CYP-treated		Irradiated	
Rf.	B. %	Rf.	B. %	Rf.	B. %	Rf.	B. %	Rf.	B. %	Rf.	B. %	Rf.	B. %
0.14	38.78	0.14	38.77	0.14	35.04	0.14	42.32	0.14	38.17	0.14	35.27	0.14	36.70
0.26	33.44	0.26	27.85	0.25	25.78	0.26	33.82	0.27	29.72	0.26	45.04	0.26	32.85
0.50	8.12	0.51	8.00	0.42	9.90	0.51	23.86	0.49	11.79	0.33	19.70	0.40	8.51
0.57	19.66	0.58	25.39	0.52	29.28	—	—	0.58	12.53	—	—	0.49	13.80
—	—	—	—	—	—	—	—	0.69	7.79	—	—	0.68	8.14

Rf.: Relative Mobility, B. %: Band Percent.
Arrangement of the bands at each lane is not correlated with the bands in the other lanes.

pattern in the testicular tissue. This may refer to inhibition in expression of the genes which are responsible for synthesis of the testicular EST. This caused structural changes of leydig and sertoli cells and hence inhibition of spermatogenesis[72]. It was reported that the 3.6-kb TESK1 mRNA was expressed predominantly in rat testicular germ cells at stages of pachytene spermatocytes to round spermatids[24,25]. Several protein kinases are phosphorylated on residues located in the activation loop. The exposure to the external deleterious factors like irradiation and the other toxic substances exhibited mutagenic effect on this protein kinase. According to the site-specific mutation analyses, it was demonstrated that TESK1 autophosphorylates Ser-215, which lies in the activation loop. The TESK1 mutant with replacement of Ser-215 by alanine has no activity to phosphorylate histone H3, which suggests that autophosphorylation of Ser-215 is required to exhibit the kinase activity of TESK1[73,74].

CONFLICTS OF INTEREST

There are none declared conflicts of interest by authors

REFERENCES

1. Liu J, Xiong CL, Shen SL. Distribution of attractin protein and mRNA in the testis of rat of different ages. Zhonghua Nan Ke Xue 2005; 11(4): 264-8.
2. Thakur SC, Thakur SS, Chaube SK, Singh SP. Subchronic supplementation of lithium carbonate induces reproductive system toxicity in male rat. Reprod. Toxicol 2003; 17(6): 683-90.
3. Aseff SG, Fuentes LB. Lithium effect on testicular tissue of adult male and female viscacha. Acta Physiol Pharmacol 1995; 45:87-95.
4. Toghyani S, Dashti GR, Roudbari NH, Rouzbehani S, Monajemi R. Lithium carbonate inducing disorders in three parameters of rat sperm. Adv Biomed Res 2013; 2 (3):55.
5. Horn MM, Ramos AR, Winkelmann L, Matte US, Goldani HA, Silveira TR. Seminiferous epithelium of rats with food restriction and carbon tetrachloride-induced cirrhosis. Invest Urologoy 2006; 32 (1):94-9.
6. Sheweita PM, El-Gabar M, Bastawy M. Carbon tetrachloride changes the activity of cytochrome P450 system in the liver of male rats: role of antioxidants. Toxicology 2001; 169 (2): 83-92.
7. Huang BM, Lai HY, Liu MY. Concentration dependency in lead-inhibited steroidogenesis in MA-10 mouse Leydig tumor cells. J Toxicol Environ Health A 2002; 65 (7): 557-567.
8. Benoff S, Centola GM, Millan C, Napolitano B, Marmar JL, Hurley IR. Increased seminal plasma lead levels adversely affect the fertility potential of sperm in IVF. Hum Reprod 2003; 18 (2): 374-383.
9. Ghelberg NW, Bordas E. Lead-induced experimental lesions of the testis and their treatment. J Appl Toxicol 1981; 1 (5): 284-6.
10. Shivakumar P, Usha Rani M, Gopala Reddy A, Anjaneyulu Y. A Study on the Toxic Effects of Doxorubicin on the Histology of Certain Organs. Toxicol Int 2012; 19(3): 241–4.
11. Bahadur G, Ozturk O, Muneer A, Wafa R, Ashraf A, Jaman N, Patel S, Oyede AW, Ralph DJ. Semen quality

before and after gonadotoxic treatment. Hum Repro 2000; 20 (3): 774-81.
12. Seski JC, Edwards CL, Gershenson DM, Copeland LJ. Doxorubicin and cyclophosphamide chemotherapy for disseminated endometrial cancer. Obstet Gynecol 1981; 58 (1):88-91.
13. Drumond AL, Weng CC, Wang G, Chiarini-Garcia H, Eras-Garcia L, Meistrich ML. Effects of multiple doses of cyclophosphamide on mouse testes: Accessing the germ cells lost, and the functional damage of stem cells. Reprod Toxicol 2011; 32 (4): 395–406.
14. Dym M, Clermont Y. Role of spermatogonia in the repair of the seminiferous epithelium following x-irradiation of the rat testis. Am J Anat 1970; 128 (3) :265–82.
15. Kangasniemi M, Veromaa TI, Kulmala J, Kaipia A, Toppari PM. DNA-flow cytometry of defined stages of rat seminiferous epithelium: effects of 3 Gv of high-energy X-irradiation. J Androl 1990; 11(3):312–7.
16. Gianni L, Salvatorelli E, Minotti G. Anthracycline cardiotoxicity in breast cancer patients: Synergism with trastuzumab and taxanes. Cardiovasc Toxicol 2007; 7 (2):67–71.
17. Naiyara A, Abdul E, Ali AA, Ahmed RA. Simavastatin cardioprotective effect in doxorubicin induced cardiotoxicity in rats. J Basic Appl Sci 2010; 6:29–38.
18. Hou M, Chrysis D, Nurmio M. Doxorubicin induces apoptosis in germ line stem cells in the immature rat testis and amifostine can not protect against this cytotoxicity. Cancer research 2005; 65 (21): 9999-10005.
19. Zanetti SR, Maldonado EN, Aveldano MI. Doxorubicin affects testicular lipids with long-chain (C18-C22) and very long-chain (C24-C32) polyunsaturated fatty acids. Cancer Res 2007; 67 (14): 6973-80.
20. Ezz MK. The Ameliorative Effect of Echinacea Purpurea Against Gamma Radiation Induced Oxidative Stress and Immune Responses in Male Rats. Australian Journal of Basic and Applied Sciences 2011; 5 (10): 506-12.
21. Schally AV, Paz-Bouza JI, Schlosser JV, Karashima T, Debeljuk L, Gandle B, Sampson M. Protective effects of analogs of luteinizing hormone-releasing hormone against x-irradiationinduced testicular damage in rats. Proc Natl Acad Sci USA 1987; 84 (3): 851–5.
22. Jagetia GC, Jyothi P, Krishnamurthy H. Effect of vindesine sulfate on the radiation-induced alterations in mouse spermatogenesis: a flow cytometric evaluation. Mutation Research 1998; 398 (1-2): 163–74.
23. Toshima J, Tanaka T, Mizuno K. Dual Specificity Protein Kinase Activity of Testis-specific Protein Kinase 1 and Its Regulation by Autophosphorylation of Serine-215 within the Activation Loop. The Journal of Biological Chemistry 1999; 274 (17): 12171–6.
24. Toshima J, Ohashi K, Okano I, Nunoue K, Kishioka M, Kuma K, Miyata T, Hirai M, Baba T, Mizuno K. Identification and Characterization of a Novel Protein Kinase, TESK1, Specifically Expressed in Testicular Germ Cells. The Journal of Biological Chemistry 1995; 270 (52): 31331–7.
25. Toshima J, Koji T, Mizuno K. Stage-specific expression of 1 (TESK1) in rat spermatogenic cells. Biochem Biophys Res Commun 1998; 249 (1): 107–12.
26. Hanks SK, Quinn AM. Protein kinase catalytic domain sequence database: identification of conserved features of primary structure and classification of family members. Methods Enzymol 1991; 200: 38–62.
27. Elgawish RA, Abdelrazek HMA. Effects of lead acetate on testicular function and caspase-3 expression with respect to the protective effect of cinnamon in albino rats. Toxicology Reports 2014; 1: 795–801.
28. Mostafa AMA, Qattan AT, Alukdsy FM, Alkorim SA. The toxic effect of lithium carbonate on the reproductive system of immature male mice. Egypt J Exp Biol (Zool) 2010; 6 (1): 141 – 9.
29. Hozayen WG. Effect of Hesperidin and Rutin On Doxorubicin Induced Testicular Toxicity in Male Rats. International Journal of Food and Nutrition Science 2012; 1 (1): 31 – 42.
30. Eidi A, Mortazavi P, Tehrani ME, Rohani AH, Safi S. Hepatoprotective effects of pantothenic acid on carbon tetrachloride-induced toxicity in rats. EXCLI Journal 2012; 11: 748-59.
31. Kanth MA, Kaur P, Ahmad B, Sharma S. Histological effect of anticancer drug cyclophosphamide (CP) on testis of *Rattus rattus*. Indo American Journal of Pharm Research 2014; 4 (05):2645-9.
32. Abulyazid I, Abdalla MS, Sharada HM, Abd El Kader MA, Kamel WM. Protective Effect of Salicin Isolated from Egyptian Willow Leaves *(Salix subserrata)* against Gamma-Radiation-Induced Electrophoretic and Molecular Changes in Epididymal Tissue in Rats. International Journal of Recent Scientific Research 2015; 6 (6): 4421-35.
33. Elshawi OE, Nabil AI, Mahmoud MF. Testicular damages mediated by oxidative stress in swiss albino rats exposed to lead acetate and gamma rays co-toxicity the possible protective role of taurine. J Appl Environ Biol Sci 2014; 4 (8):279-91.
34. Bradford MM. A rapid and sensitive method for the quantitation of microgram quantities of protein utilizing the principle of protein-dye binding. Anal Biochem 1976; 72 (1-2): 248-54.
35. Laemmli UK. Cleavage of structural proteins during the assembly of the head of Bacteriophage T4. Nature 1970; 227: 680-5.
36. Darwesh OM, Moawad H, Barakat OS, Abd El-Rahim WM. Bioremediation of Textile Reactive Blue Azo Dye Residues using Nanobiotechnology Approaches. Research Journal of Pharmaceutical, Biological and Chemical Sciences 2015; 6 (1): 1202-11.
37. Subramaniam HN, Chaubal KA. Evaluation of intracellular lipids by standardized staining with a Sudan black B fraction. J Biochem Biophys Methods 1990; 21 (1):9-16.
38. Siciliano MJ, Shaw CR. Separation and visualization of enzymes on gels, in Chromatographic and

Electrophoretic Techniques, Vol. 2, Zone Electrophoresis, Smith, I., Ed., Heinemann, 1976; London, p. 185.
39. Rescigno A, Sanjust E, Montanari L, Sollai F, Soddu G, Rinaldi AC, Oliva S, Rinaldi A. Detection of laccase, peroxidase and polyphenol oxidase on a single polyacrylamide gel electrophoresis. Anal Lett 1997; 30 (12): 2211-20.
40. Ahmad A, Maheshwari V, Ahmad A, Saleem R, Ahmad R. Observation of esterase-like-albumin activity during N'- nitrosodimethyl amine induced hepatic fibrosis in a mammalian model. Maced J Med Sci 2012; 5 (1): 55–61.
41. Park J, Karplus K, Barrett C, Hughey R, Haussler D, Hurbbard T, Chothia C. Sequence comparisons using multiple sequences detect three times as many remote homologues as pairwise methods. J Mol Biol 1998; 284 (4): 1201-10.
42. Lindahl E, Elofsson A. Identification of related proteins on family, superfamily and fold level. J Mol Biol 2000; 295 (3) : 613-25.
43. Soding J. Protein homology detection by HMM-HMM comparison. Bioinformatics 2005; 21 (7): 951-60.
44. Zhang Y, Skolnick J. The protein structure prediction problem could be solved using the current PDB library. Proc Natl Acad Sci USA 2005; 102 (4): 1029-34.
45. Bowie JU, Luthy R, Eisenberg D. A method to identify protein sequences that fold into a known three-dimensional structure. Science 1991; 253(5016):164-70.
46. Bryant SH, Altschul SF. Statistics of sequence-structure threading. Curr Opin Struct Biol 1995; 5 (2) : 236-44.
47. Jones DT. GenTHREADER: an efficient and reliable protein fold recognition method for genomic sequences. J Mol Biol 1999; 287 (4): 797-815.
48. Hermans J, Berendsen HJC, van Gunsteren WF, Postma JPM. A consistent empirical potential for water–protein interactions. Biopolymers 1984; 23 (8): 1513-8.
49. Weiner SJ, Kollman PA, Case DA, Singh UC, Ghio C, Alagona G, Profeta S, Weiner P. A new force field for molecular mechanical simulation of nucleic acids and proteins. J Am Chem Soc 1984; 106 (3):765–84.
50. Kale´ L, Skeel R, Bhandarkar M, Brunner R, Gursoy A, Krawetz N, Phillips J, Shinozaki A, Varadarajan K, Schulten K. NAMD2: Greater scalability for parallel molecular dynamics. J Comput Phys 1999; 151: 283-312.
51. Price SL. Toward more accurate model of intermolecular potentials for organic molecules. Rev Comput Chem 2000; 14: 225-89.
52. Giometti CS, Gemmell MA, Nance SL, Tollaksen SL, Taylor J. Detection of heritable mutations as quantitative changes in protein expression. J Biol Chem 1987; 262 (26): 12764 –7.
53. Abdalla MS, Sharada HM, Abulyazid I, Abd El Kader MA, Kamel WM. Ameliorative effect of salicin against gamma irradiation induced electrophoretic changes in brain tissue in male rats. UK Journal of Pharmaceutical and Biosciences 2015; 3(2): 29-41.
54. Sharada HM, Abdalla MS, Ibrahim IA, El Kader MA, Kamel WM. Electrophoretic study of the antagonistic effect of salicin isolated from Egyptian willow leaves (*Salix subserrata*) against the effect of gamma irradiation in male rats. World Journal of Pharmacy and Pharmaceutical Sciences 2015; 4(05): 1576-1602.
55. Cho Y, Song KB. Effect of g-irradiation on the molecular properties of BSA and b-lactoglobulin. J Biochem Mol Biol 2000; 33: 133-7.
56. Guasch R, Renaupiqueras J, Guerri C. Chronic ethanol-consumption induces accumulation of proteins in the liver Golgi apparatus and decreases galactosyltransferase activity. Alcohol Clin Exp Res 1992; 16 (5): 942–8.
57. Mathur N, Pandey G, Jain GC. Male Reproductive Toxicity of Some Selected Metals: A Review. Journal of Biological Sciences 2010; 10 (5): 396-404.
58. Joshi DK, Chauhan DS, Pathak AK, Mishra S, Choudhary M, Singh VP, Tripathi S. Lithium potentiate oxidative burden and reduced antioxidant status in different rat organs system. Int J Toxicol Pharm Res 2013; 5(1):9–14.
59. Toplan S, Ozdemir S, Tanriverdi G, Akyolcu MC, Ozcelik D, Darıyerli N. The Effects of Lithium Administration on Oxidant/Antioxidant Status in Rats: Biochemical and Histomorphological Evaluations. Biological Trace Element Research 2016; 169 (2): 279–84.
60. Terzi EH, Kükner A, Öztürk S, Özogul C, Üyetürk U. The Effect of Heparin on the Carbon Tetrachloride Induced Changes in Rat Testis. Acta Medica Anatolia 2014; 2 (2): 56-9.
61. Abraham P, Wilfred G, Cathrine. Oxidative damage to the lipids and proteins pf the lungs, testis and kidney of rats during carbon tetrachloride intoxication. Clin Chim Acta 1999; 289 (1-2): 177-9.
62. Patil RL, Balaraman R. Effect of melatonin on doxorubicin induced testicular damage in rats. Int J Pharma Tech Res 2009; 1 (3):879–84.
63. De Beer EL, Bottone AE, Voest EE. Doxorubicin and mechanical performance of cardiac trabeculae after acute and chronic treatment: A review. Eur J Pharmacol 2001; 415 (1):1–11.
64. Moon S, Song KB. Effect of gamma-irradiation on the molecular properties of ovalbumin and ovomucoid and protection by ascorbic acid. Food Chem 2001; 74: 479-83.
65. Lai H, Singh N. Single and double strand DNA Breaks in rat brain cells after acute exposure to radio-frequency electromagnetic radiation. International Journal of Radiation Biology 1996; 69(4): 513-21.
66. Teng TY, Moffat K. Primary radiation damage of protein crystals by an intense synchrotron X- ray beam. Journal of Synchrotron Radiation 2000; 7 (Pt 5): 313 - 7.
67. Arenas-Ríos E, León-Galván MA, Mercado PE, López-Wilchis R, Cervantes DLMI, Rosado A. Superoxide dismutase, catalase, and glutathione peroxidase in the

testis of the Mexican big-eared bat (*Corynorhinus mexicanus*) during its annual reproductive cycle. Comparative Biochemistry and Physiology Part A: Molecular & Integrative Physiology 2007; 148 (1): 150-8.

68. Aly HAA, Domènech Ò, Banjar ZM. Effect of nonylphenol on male reproduction: Analysis of rat epididymal biochemical markers and antioxidant defense enzymes. Toxicology and Applied Pharmacology 2012; 261 (2): 134-41.
69. Manciluae S, Giurgea R, Ilyes I. Biochemical changes in white rats subjected to sublethal irradiation. Radiobiol Radiother 1978; 19 (3): 331-6.
70. Tawa R, Kimura Y, Komura J, Miyamura Y, Kurishita A, Sasaki MS, Sakurai H, Ono T. Effects of X-ray irradiation on genomic DNA methylation levels in mouse tissues. J Radiat Res (Tokyo) 1998; 39(4): 271−8.
71. Masters J, Holmes S. Isoenzymes and ontogeny. Bio Rev 1972; 47 (3): 309-61.
72. Mikhailov AT, Torrado M. Carboxylesterases moonlight in the male reproductive tract: a functional shift pivotal for male fertility. Frontiers in Bioscience 2000; 5:E53-62.
73. Steinberg RA, Clauthron RD, Symcox MM, Shuntoh H. Autoactivation of catalytic (C alpha) subunit of cyclic AMP-dependent protein kinase by phosphorylation of threonine 197. Mol Cell Biol 1993; 13 (4): 2332–41.
74. Johnson LN, Noble MEM, Owen DJ. Active and inactive protein kinases: structural basis for regulation. Cell 1996; 85 (2): 149–58.